

Hydrogen-Bonded Cholesteric Liquid Crystals—A Modular Approach Toward Responsive Photonic Materials

Florian Malotke, Matthias Spengler, Lukas Pschyklenk, Marco Saccone, Peter Kaul, and Michael Giese*

A supramolecular approach for photonic materials based on hydrogen-bonded cholesteric liquid crystals is presented. The modular toolbox of low-molecular-weight hydrogen-bond donors and acceptors provides a simple route toward liquid crystalline materials with tailor-made thermal and photonic properties. Initial studies reveal broad application potential of the liquid crystalline thin films for chemo- and thermosensing. The chemosensing performance is based on the interruption of the intermolecular forces between the donor and acceptor moieties by interference with halogen-bond donors. Future studies will expand the scope of analytes and sensing in aqueous media. In addition, the implementation of the reported materials in additive manufacturing and printed photonic devices is planned.

1. Introduction

Supramolecular chemistry provides a powerful approach toward responsive materials, since it relies on the reversibility of non-covalent interactions. This allows a dynamic reorganization of the supramolecular structure as response to external stimuli such as changes in the temperature, irradiation with light, or the presence of analytes interfering with the preexisting intermolecular forces between the building blocks of the material.^[1,2] With respect to the design of hydrogen-bonded liquid crystals

(HB LCs), Kato and Fréchet performed pioneering work using the complementary interaction between benzoic acid groups and pyridyl derivatives.^[3–15] Later, Bruce and coworkers studied related mesogens and demonstrated that phenol derivatives are suitable proton-donating candidates to introduce liquid crystallinity.^[16,17] This group reported also the first halogen-bonded LCs, which started a new field in the design of supramolecular liquid crystals.^[18–20]

Since 2016, our group has been working on hydrogen-bonded and halogen-bonded liquid crystals.^[21–24] Therefore, we employ a modular approach, which allows comprehensive structure–property relationship


studies as well as systematic tuning of the properties of the obtained functional assemblies (see Scheme 1a).^[25–29] Recently, we focused on the development of responsive photonic materials based on cholesteric liquid crystals (CLCs).^[30] CLCs represent 1D photonic structures, which selectively reflect light of a specific handedness and wavelength (selective reflection band, SRB), when the helical pitch is within the region of the wavelength of visible light (according to Bragg's law, see Scheme 1b). CLCs are promising for sensing applications as they are independent from energy sources, easy to read out, and easy to prepare.^[31] Within the past decade, several groups reported a series of CLC sensors based on polymeric liquid crystalline networks. For instance, Schenning and coworkers combined several acrylate-based monomers to create printable cholesteric liquid crystalline networks. Since these networks rely partly on crosslinking by hydrogen bonding, they optically respond to the presence of hydrogen-bond donating or accepting analytes as well as to changes in the pH.^[31–34] Studies using low-molecular-weight, hydrogen-bonded CLCs for photonic sensing are rarely found in literature.^[35–38]

Based on our previous findings and inspired by the seminal work on HB LCs by Bruce and coworkers, we herein report a modular toolbox for photonic materials responding to changes in temperature and chemical vapors. In contrast to previous reports based on liquid crystalline polymer networks or where the supramolecular entity is used as dopand in a commercially available liquid crystalline host, we herein report the first series of liquid crystalline materials, exclusively relying on supramolecular assemblies^[39–41] and investigated their photonic behavior. The major advantage of this modular strategy is its versatility and the easy accessibility of new materials compared to the

F. Malotke, M. Spengler, M. Giese
Organic Chemistry and Center for Nanointegration Duisburg-Essen
(CENIDE)
University Duisburg-Essen
Universitätsstraße 7, 45141 Essen, Germany
E-mail: michael.giese@uni-due.de

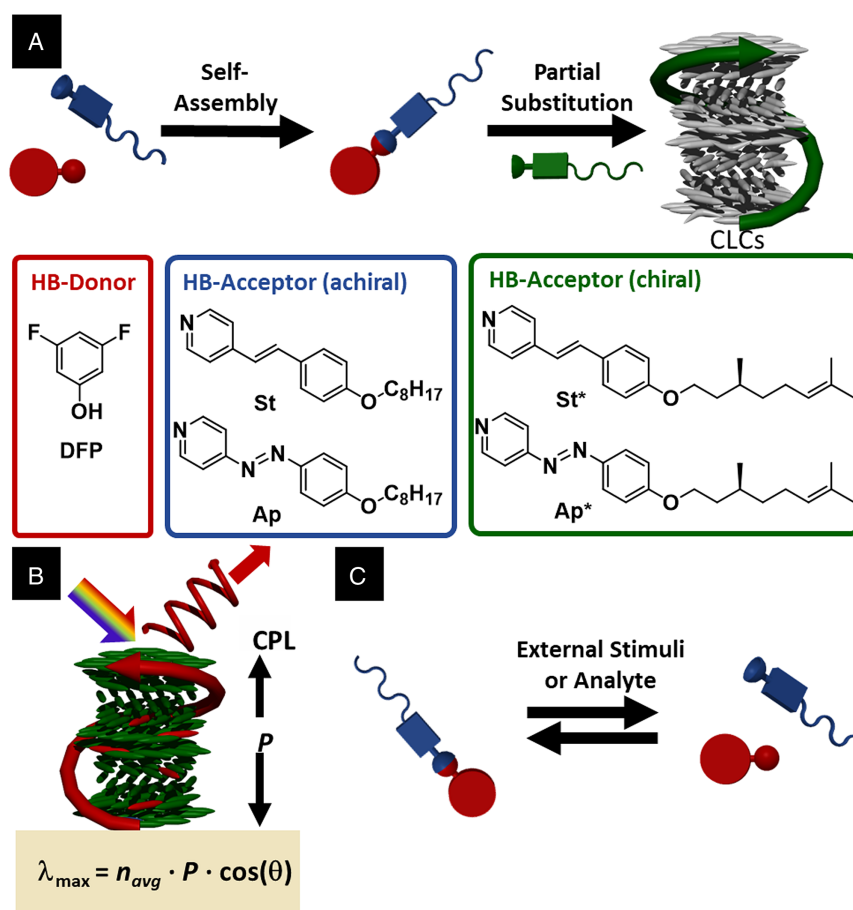
L. Pschyklenk, P. Kaul
Institute of Safety and Security Research
University of Applied Sciences Bonn-Rhein-Sieg
53359 Rheinbach, Germany

M. Saccone
Dipartimento di Ingegneria
Università degli Studi di Palermo
Viale delle Scienze, Ed. 6, Palermo 90128, Italy

 The ORCID identification number(s) for the author(s) of this article can be found under <https://doi.org/10.1002/adpr.202100353>.

© 2022 The Authors. Advanced Photonics Research published by Wiley-VCH GmbH. This is an open access article under the terms of the Creative Commons Attribution License, which permits use, distribution and reproduction in any medium, provided the original work is properly cited.

DOI: 10.1002/adpr.202100353



Scheme 1. Schematic representation of the modular approach toward hydrogen-bonded cholesteric liquid crystals (CLCs). a) Partial substitution of the achiral hydrogen-bonded (HB) acceptor (blue) by a chiral analogue (green) yields CLCs reflected visible light. b) Helical structure leading to a selective reflection of circularly polarized light with a wavelength equivalent to the length of the helical pitch (P), the average refractive index of the material (n_{avg}) and the angle of incidence (θ) of the incident light beam. Scheme visualizing the sensing principle of the hydrogen-bonded CLCs. c) The external stimuli or analyte will interfere with the hydrogen bonding and yield a change in the helical photonic structure.

well-known polymeric systems. By self-assembly of the supramolecular building blocks, a plethora of new materials with tailor-made properties is accessible. In addition, since the materials are based on low-molecular-weight mesogens, the response times are several orders of magnitudes faster. For our initial studies, we prepared a library of stilbazole (St) and azopyridine-based (Ap) hydrogen-bond acceptors and combined them with 3,5-difluorophenol (DFP) to obtain the hydrogen-bonded liquid crystalline hosts. By partial substitution of the hydrogen bond-accepting moiety by their chiral analogue (St* and Ap*), four different cholesteric liquid crystalline systems were obtained (DFP(St*_{50%}/St_{50%}), DFP(Ap*_{50%}/St_{50%}), DFP(St*_{50%}/Ap_{50%}), and DFP(Ap*_{50%}/Ap_{50%}), see Scheme 1).

2. Results and Discussion

2.1. Liquid Crystalline Properties

To investigate the potential and properties of the selected library for sensing applications, we initially studied the liquid crystalline

properties of the four different compositions. The formation of the hydrogen-bonded assemblies was proven by Infrared (IR) spectroscopy (see electronic supplementary information (ESI) for details) and is indirectly supported by the formation of liquid crystalline assemblies (the individual building blocks do not show liquid crystalline behavior) as proven by polarized optical microscopy (POM) (see Figure 1a–c). All investigated compositions form monotropic chiral nematic phases. A comparison of the mesomorphic behavior of the assemblies revealed that the systems hosted by the achiral Ap...DFP assemblies tend to recrystallize at temperatures of $\approx 35^\circ\text{C}$, while the crystallization of the St...DFP-doped systems is suppressed, preserving liquid crystallinity up to several weeks. Moreover, after eventually crystallizing, the liquid crystalline properties and structural coloration can be recovered by remelting the assembly. Thus, the latter systems appear promising for the development of CLC sensor at room temperature.

The color of light reflected by the CLCs depends on the concentration and the helical twisting power (HTP) of chiral dopant added to the achiral host system. To control the initial color of the CLC films, it is crucial to determine the HTP of

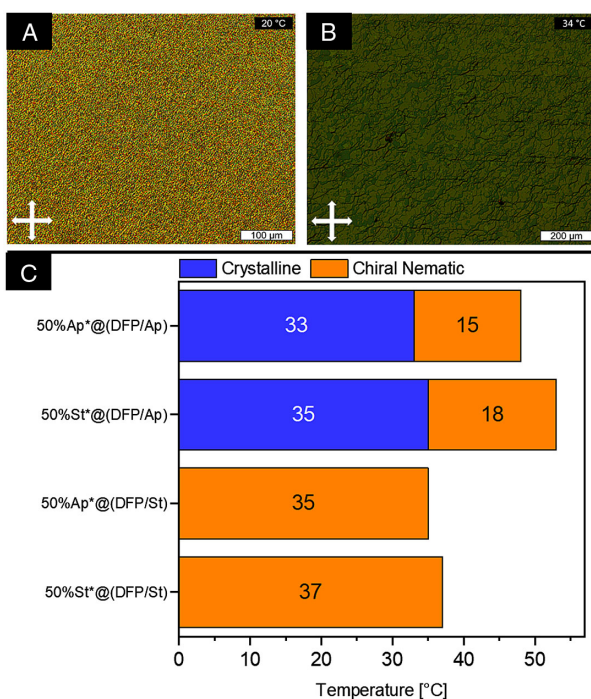


Figure 1. Representative polarized optical microscopy (POM) images for a) 3,5-difluorophenol (DFP)(St*50%/St50%) and b) DFP(Ap*50%/St50%) showing the typical nonaligned and aligned textures of a chiral nematic phase as well as c) a summary of transition temperatures of the four chiral liquid crystalline assemblies as determined by POM.

the chiral dopants (for detailed procedure, see ESI Chapter 4). The HTP (β) is determined by the enantiomeric excess (ee), the dopant concentration (Dopant), and the helical pitch of the chiral nematic phase (P).

$$\beta = (P * [\text{Dopant}] * ee)^{-1} \quad (1)$$

The HTP values for DFP...Ap*@(DFP...St and DFP...St*@(DFP...St were found to be in the same region 4.5 ± 0.2 and $3.9 \pm 0.1 \mu\text{m}^{-1}$, respectively. Based on these results, we extrapolated the ratio of chiral to achiral hydrogen-bonded liquid crystal to obtain green/blue CLC films at room temperature. Subsequently, the CLC films were prepared by application of the material to a black polypropylene substrate via shearing with a glass slide. The samples show a reversible color change as a response to changes in the temperature, which is well-known behavior for CLC materials.^[42] However, to our surprise, the thermal response of DFP(Ap*50%/St50%) is significantly different from its analogue where the chiral azopyridine Ap* is exchanged by the chiral stilbazole St*. While the DFP(Ap*50%/St50%) films showed a strong and prompt response to changes in the temperature, the temperature response of the DFP(St*50%/St50%) appeared less pronounced.

2.2. Temperature Response

To investigate the thermal response of the Ap*-based system in more detail, the concentration of the chiral dopant has been

increased to adjust to a blue reflecting color. The fast and reversible change in the reflection color of the DFP(Ap*55%/St45%) films can easily be followed by the naked eye (see Figure 2a–c). To quantify the thermosensing behavior, the reflection spectra were recorded as a function of the temperature. Initially, the films appear green/blue at 27 °C with an SRB maximum at 470 nm. Upon cooling, the color of the films immediately red-shifts with an SRB maximum at 645 nm at 10 °C (see Figure 2d).^[43] Below 10 °C the reflection band shifts into the IR-region and the films appear colorless and opaque. In contrast, temperatures above 30 °C yield a transition from the mesophase to the isotropic phase leading to a vanishing of the structural color of chiral nematic phase. To show the fast and reversible response of the CLC films to temperature changes, the heating and cooling cycles were repeated showing that at least for five repetitions no significant hysteresis was observed (see Figure 2e).

In contrast to the DFP(Ap*55%/St45%) sample, thin films of DFP(St*55%/St45%) showed a less pronounced response to temperature changes, which we attribute to stronger intermolecular forces in this system resulting in a thermally more robust photonic structure.^[44] Therefore, this system was tested with respect to its chemosensing ability.

2.3. Analyte Sensing in Gaseous Phase

As our initial aim for the present study with hydrogen-bonded assemblies was to investigate their use in photonic sensing of vapors and gases, we tested the response to vapors of a series of hydrogen-bond donors and acceptors. To our surprise, analytes such as water or ammonia vapors did not show a significant effect on the coloration of the CLC films ($\Delta\text{SRB} = 25 \text{ nm}$, see ESI Figure S17, Supporting Information). We attribute this behavior to an incompatibility issue between the polar analytes and the hydrophobic CLC films. In contrast, halogens such as iodine appear to be promising analytes since they are nonpolar and are able to form halogen bonds to the pyridyl-based acceptor moieties. Indeed, the presence of iodine vapors yielded a prompt redshift of the SRB, which was visible by the naked eye (see Figure 3a,b). Previously, we reported the photonic NO₂ gas sensing by binaphthyl diimine metal complexes as reactive dopants in E7.^[30] Here, we used the same experimental setup to quantify the gas-sensing performance of the hydrogen-bonded CLC films (for further details, see ESI Chapter 6.1). The setup allows to continuously record reflection spectra of the investigated CLC films while exposed to analyte vapors (see Figure S15, Supporting Information). The sample chamber was flushed with synthetic air for several minutes before exposing the sample to iodine vapors. The photonic response of the CLC films was followed by measuring the shift of the reflectance peak maximum ($\Delta\lambda_{\text{max}}$) as a function of time (s). The measurements clearly show a fast and direct response of the films when exposed to iodine vapors at 600 s, yielding a strong redshift from 590 to 660 nm within 300 s. As soon as the iodine concentration within the carrier gas drops at 1000 s, the shift of the SRB maximum is reversed returning to 600 nm with a slight hysteresis (see Figure 3c and Figure S16, Supporting Information).

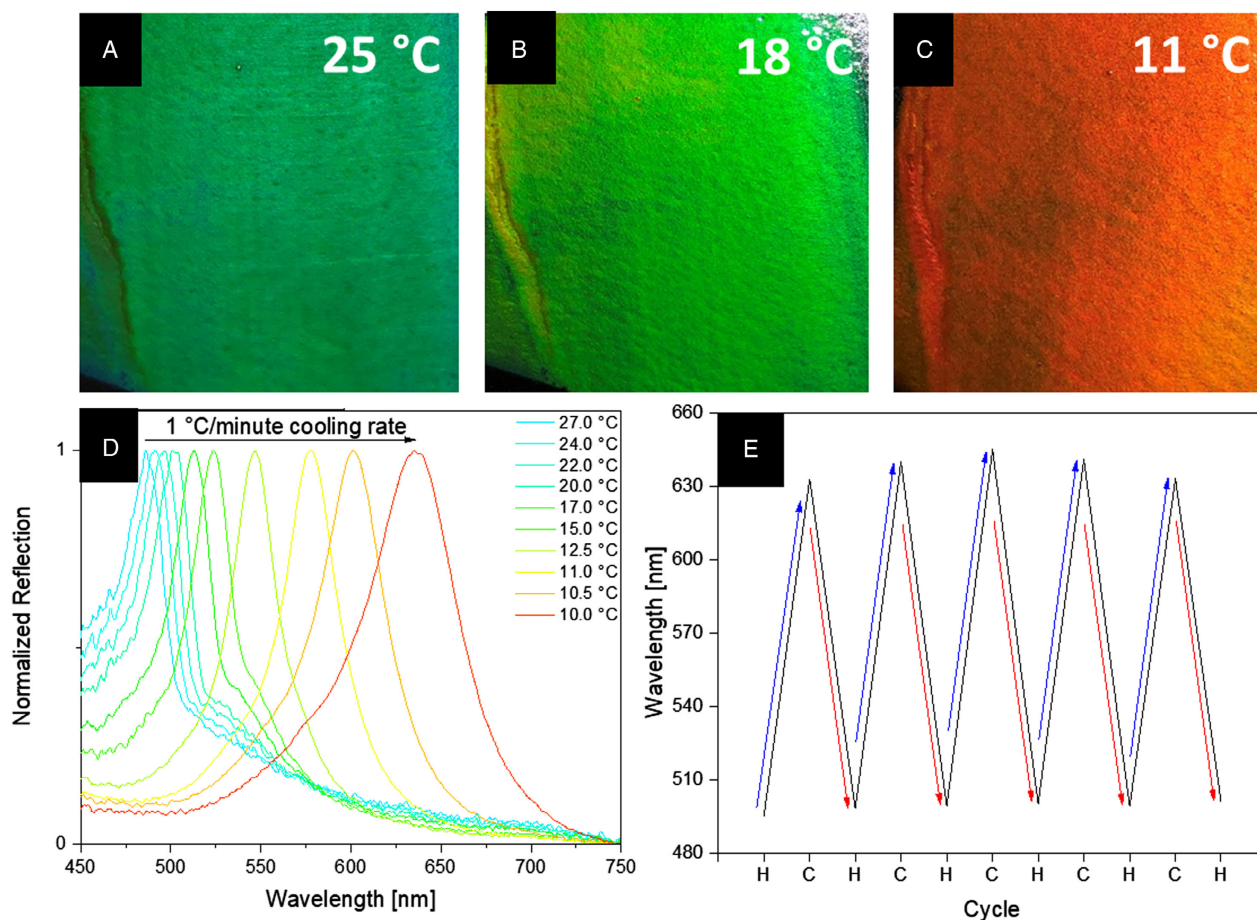


Figure 2. Demonstration of the temperature-dependant shift of the selective reflection band (SRB) of thin Hydrogen-bonded liquid crystals (HB LC) film (DFP(Ap*55%/St45%)) a) at ≈ 25 °C (ambient temperature), b) at 18 °C, and c) at 11 °C. Measurement of the SRB for the very same sample at a 1 °C min^{-1} cooling gradient, revealing a significant d) redshift of the SRB of about 175 nm. e) Repeating heating/cooling cycles between room temperature and 10 °C demonstrating a persistent thermoresponsive effect.

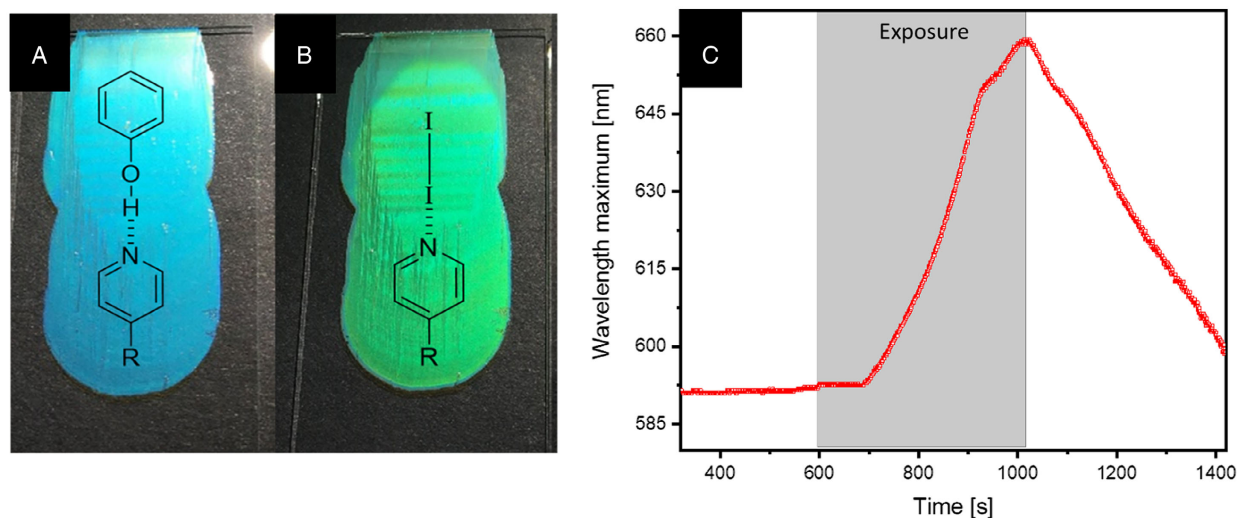


Figure 3. A continuous redshift of the SRB maximum can be recognized, followed by a blue shift, indicating reversibility. Hydrogen-bonded complex a) before and b) after 3 s exposure to an iodine vapor-containing chamber redshifting the SRB after iodine incorporation. c) Time-resolved reflectance measurement of the SRB maximum of DFP(St*55%/St45%) upon exposure to iodine vapors, exhibiting a redshift of 70 nm within 300 s.

We attribute the strong and reversible shift of the SRB to the disruption of the hydrogen bond between the DFP and the hydrogen bond-donating group by iodine, followed by a reorganization of the cholesteric mesophase yielding a change in the helical pitch. To prove our hypothesis, we first determined the HTP value of an $I_2 \cdots St^*$ assembly in DFP $\cdots St$ and compared these to the previously obtained HTP values for DFP $\cdots St^*$. Indeed, the HTP of the iodine assembly is significantly lower ($2.1 \pm 0.1 \mu m^{-1}$) than the one for DFP $\cdots St^* @ DFP \cdots St$ ($4.0 \pm 0.1 \mu m^{-1}$), which would explain the redshift of the SRB maximum (see ESI Figure S12, Supporting Information). In the next step, we calculated the interaction strengths of the DFP $\cdots St$ and $I_2 \cdots St$ and found that the halogen and the hydrogen bonds are comparable in their strength (-11.96 and $-10.90 \text{ kcal mol}^{-1}$, respectively) supporting our assumption that the halogen bond to the iodine is a serious competitor and promotes a disruption of the hydrogen bond to the DFP (see ESI Figure S24 and S25, Supporting Information). Finally, the CLC films were investigated by attenuated total reflection infrared spectroscopy during the exposure to iodine (see ESI Figure S19–S21, Supporting Information). The IR spectra clearly show that the well-defined band of the phenolic OH-group in the assembly at 2634 cm^{-1} vanishes upon exposure to iodine vapors, and broad signal of the nonbonded phenol occurs around 3259 cm^{-1} . These results demonstrate that the phenol is partly replaced by the iodine in the assemblies.

Since the DFP(Ap $^{*55\%}/St_{45\%}$) contains the photo-switchable azopyridine moieties, we were interested in the impact of irradiation on the structural coloration of the CLC films (for details, see ESI Chapter 7/Figure S22, Supporting Information).^[43] Therefore, the CLC films were irradiated with a laser pointer (405 nm, 5 mW, 2 s), and the reflection spectra were recorded before and after irradiation at room temperature. The reflectance shift, however, is rather unsatisfying shifting from initially 595–585 nm upon irradiation (see Figure S23, Supporting Information). Since the reflectance reverts back into the initial state within 10 s one cannot make a clear statement on whether the effect is a thermal one or solely driven by a photo-isomerization process.

3. Conclusion

In conclusion, we presented a modular tool box to form CLC films based on low-molecular-weight, hydrogen-bonded liquid crystalline assemblies. By variation of the employed hydrogen-bond acceptors (chiral or achiral), four sensor systems were developed with significantly differing mesomorphic properties and sensing capability, while the systems based on DFP $\cdots Ap$ turned out to crystallize already at a temperature of $35^\circ C$ making them unappealing for applications. In contrast, DFP $\cdots St$ host appears promising for the development of thermo- and chemo-responsive materials. The CLC films of DFP $\cdots Ap^* @ DFP \cdots St$ are sensitive thermosensors in the temperature range between 10 and $27^\circ C$, while the CLC films of the closely related DFP $\cdots St^* @ DFP \cdots St$ system appear to be less sensitive to temperature changes. However, in a first attempt, we were able to show that these systems can be used to sense iodine vapors, while water vapor did not yield in a significant

change of the structural color (see ESI Figure S17, Supporting Information). The investigation of the photo-response of the system DFP $\cdots Ap^* @ DFP \cdots St$ revealed a small shift of the reflectance maximum, which quickly reversed back to its initial value. Further studies will be conducted in the future to improve the photo-switching performance of the hydrogen-bonded CLC films and to broaden the scope of relevant analytes for chemosensing. In addition, we will improve the processability of the materials toward their use in additive manufacturing or printed photonic devices.

Supporting Information

Supporting Information is available from the Wiley Online Library or from the author.

Acknowledgements

F.M. and M.G. gratefully thank the DFG for the financial support. M.G. gratefully acknowledges the Professor-Werdelmann foundation. L.P. and P.K. acknowledge the financial support of the project OptoSpin (FKZ 13FH023IX6) by the Federal Ministry of Education and Research of Germany. M. S. acknowledges PON R&I 2014-2020—AIM (Attraction and International Mobility), project AIM 1813040 for financial support.

Open Access funding enabled and organized by Projekt DEAL.

[Correction added on May 2, 2022, after first online publication: Projekt DEAL funding statement has been added.]

Conflict of Interest

The authors declare no conflict of interest.

Data Availability Statement

The data that support the findings of this study are available from the corresponding author upon reasonable request.

Keywords

chemosensing, cholesteric phase, halogen bonding, hydrogen bonding, photonic sensing, supramolecular liquid crystals, thermosensing

Received: November 22, 2021

Revised: January 19, 2022

Published online: February 22, 2022

- [1] K. Liu, Y. T. Kang, Z. Q. Wang, X. Zhang, *Adv. Mater.* **2013**, *25*, 5530.
- [2] J. Vapaavuori, C. G. Bazuin, A. Priimagi, *J. Mater. Chem. C* **2018**, *6*, 2168.
- [3] T. Kato, T. Kato, J. M. Fréchet, T. Uryu, F. Kaneuchi, C. Jin, J. M. Fréchet, *Liq. Cryst.* **2006**, *33*, 1429.
- [4] J.-M. Lehn, *Science* **2002**, *295*, 2400.
- [5] M. Suarez, J. M. Lehn, S. C. Zimmerman, A. Skoulios, B. Heinrich, *J. Am. Chem. Soc.* **1998**, *120*, 9526.
- [6] T. Kato, J. M. Fréchet, *J. Am. Chem. Soc.* **1989**, *111*, 8533.
- [7] M. J. Brienne, J. Gabard, J. M. Lehn, I. Stibor, *J. Chem. Soc., Chem. Commun.* **1989**, 1868.
- [8] T. Kato, *Science* **2002**, *295*, 2414.

- [9] T. Kato in *Molecular Self-Assembly Organic Versus Inorganic Approaches*, Springer, New York **2000**, pp. 95–146.
- [10] K. Willis, J. E. Luckhurst, D. J. Price, J. M. J. Frechet, H. Kihara, T. Kato, G. Ungar, D. W. Bruce, *Liq. Cryst.* **1996**, *21*, 585.
- [11] D. J. Price, H. Adams, D. W. Bruce, *Mol. Cryst. Liq. Cryst. Sci. Technol., Sect. A* **1996**, *289*, 127.
- [12] H. Kihara, T. Kato, T. Uryu, S. Ujiie, U. Kumar, J. M. J. Frechet, D. W. Bruce, D. J. Price, *Liq. Cryst.* **1996**, *21*, 25.
- [13] T. Kato, H. Kihara, U. Kumar, T. Uryu, J. M. Fréchet, *Angew. Chem. Int. Ed.* **1994**, *33*, 1644.
- [14] T. Kato, H. Adachi, A. Fujishima, J. M. J. Frechet, *Chem. Lett.* **1992**, *21*, 265.
- [15] T. Kato, J. M. J. Frechet, *Macromolecules* **1989**, *22*, 3818.
- [16] D. W. Bruce, D. J. Price, *Adv. Mater. Opt. Electron.* **1994**, *4*, 273.
- [17] D. J. Price, T. Richardson, D. W. Bruce, *J. Chem. Soc., Chem. Commun.* **1995**, 1911.
- [18] H. L. Nguyen, P. N. Horton, M. B. Hursthouse, A. C. Legon, D. W. Bruce, *J. Am. Chem. Soc.* **2004**, *126*, 16.
- [19] D. W. Bruce, P. Metrangolo, F. Meyer, T. Pilati, C. Präsang, G. Resnati, G. Terraneo, S. G. Wainwright, A. C. Whitwood, *Chem. Eur. J.* **2010**, *16*, 9511.
- [20] D. W. Bruce, P. Metrangolo, F. Meyer, C. Präsang, G. Resnati, G. Terraneo, A. C. Whitwood, *New J. Chem.* **2008**, *32*, 477.
- [21] P. Metrangolo, C. Präsang, G. Resnati, R. Liantonio, A. C. Whitwood, D. W. Bruce, *Chem. Commun.* **2006**, 3290.
- [22] L. González, N. Gimeno, R. M. Tejedor, V. Polo, M. B. Ros, S. Uriel, J. L. Serrano, *Chem. Mater.* **2013**, *25*, 4503.
- [23] L. J. McAllister, C. Präsang, J. P. W. Wong, R. J. Thatcher, A. C. Whitwood, B. Donnio, P. O'Brien, P. B. Karadakov, D. W. Bruce, *Chem. Commun.* **2013**, *49*, 3946.
- [24] M. Pfletscher, C. Wölper, J. S. Gutmann, M. Mezger, M. Giese, *Chem. Commun.* **2016**, *52*, 8549.
- [25] M. Pfletscher, S. Hölscher, C. Wölper, M. Mezger, M. Giese, *Chem. Mater.* **2017**, *29*, 8462.
- [26] M. Pfletscher, J. Wysoglad, J. S. Gutmann, M. Giese, *RSC Adv.* **2019**, *9*, 8444.
- [27] M. Pfletscher, M. Mezger, M. Giese, *Soft Matter* **2018**, *14*, 6214.
- [28] M. Saccone, M. Pfletscher, S. Kather, C. Wölper, C. Daniliuc, M. Mezger, M. Giese, *J. Mater. Chem. C* **2019**, *7*, 8643.
- [29] M. Saccone, M. Spengler, M. Pfletscher, K. Kuntze, M. Virkki, C. Wölper, R. Gehrke, G. Jansen, P. Metrangolo, A. Primagi, M. Giese, *Chem. Mater.* **2019**, *31*, 462.
- [30] M. Spengler, L. Pschyklenk, J. Niemyer, P. Kaul, M. Giese, *Adv. Opt. Mater.* **2021**, *9*, 2001828.
- [31] C.-K. Chang, C. M. W. Bastiaansen, D. J. Broer, H.-L. Kuo, *Adv. Funct. Mater.* **2012**, *22*, 2855.
- [32] C.-K. Chang, C. W. M. Bastiaansen, D. J. Broer, H.-L. Kuo, *Macromolecules* **2012**, *45*, 4550.
- [33] J. E. Stumpel, C. Wouters, N. Herzer, J. Ziegler, D. J. Broer, C. W. M. Bastiaansen, A. P. H. J. Schenning, *Adv. Opt. Mater.* **2014**, *2*, 459.
- [34] F.-J. Chen, J.-B. Guo, O.-Y. Jin, J. Wei, *Chin. J. Polym. Sci.* **2013**, *31*, 630.
- [35] D. A. Winterbottom, R. Narayanaswamy, I. M. Raimundo Jr, *Sens. Actuator B Chem.* **2003**, *90*, 52.
- [36] T. J. White, M. E. McConney, T. J. Bunning, *J. Mater. Chem.* **2010**, *20*, 9832.
- [37] A. Mujahid, H. Stathopoulos, P. A. Lieberzeit, F. L. Dickert, *Sensors* **2010**, *10*, 4887.
- [38] M. Roohnikan, M. Ebrahimi, S. R. Ghaffarian, N. Tamaoki, *Liq. Cryst.* **2013**, *40*, 314.
- [39] M. Moirangthem, R. Arts, M. Merx, A. P. H. J. Schenning, *Adv. Funct. Mater.* **2016**, *26*, 1154.
- [40] H. Wang, H. K. Bisoyi, L. Wang, A. M. Urbas, T. J. Bunning, Q. Li, *Angew. Chem. Int. Ed.* **2018**, *57*, 1627.
- [41] Y. Uchida, K. Suzuki, R. Tamura, *J. Phys. Chem. B* **2012**, *116*, 9791.
- [42] F. Malotke, M. Saccone, C. Wölper, R. Y. Dong, C. A. Michal, M. Giese, *Mol. Syst. Den. Eng.* **2020**, *5*, 1299.
- [43] L. Pschyklenk, T. Wagner, A. Lorenz, P. Kaul, *ACS Appl. Polym. Mater.* **2020**, *2*, 1925.
- [44] D.-Y. Kim, K.-U. Jeong, *Liq. Cryst. Today* **2019**, *28*, 34.